Editorial

Professional Health Journal (PHJ)
https://www.ojsstikesbanyuwangi.com/index.php/PHJ/index
OPEN ACCESS

Antimycobacterial Potential of Otok-otok Leaf (Flemingia strobilifera) Extract: An In Silico and In Vitro Study

Ardhi Khoirul Hakim [a]* | Ani Qomariyah [b]

[a,b] Department of Medical Laboratory Technology, Dr. Soekardjo University

***Corespondence:**
ardhikhoirul@stikesbanyuwangi.ac.id

Volume 8(2), 709-725

https://doi.org/10.54832/phj.v8i2.1518
e-ISSN 2715-6249

Received : June 12, 2026
Revised : July 28, 2026
Accepted : August 1, 2026

ABSTRACT

Background: *Tuberculosis (TB) remains a major global health challenge due to the emergence of drug-resistant strains and the limited availability of novel antitubercular agents. Natural products have gained increasing attention as potential sources of antimycobacterial compounds. Flemingia strobilifera is known to contain diverse bioactive metabolites that may exhibit inhibitory activity against mycobacterial targets.*
Objective: *This study aimed to evaluate the antimycobacterial potential of Otok-otok (Flemingia strobilifera) leaf extract through integrated in silico and in vitro approaches.*
Methods: *Five dominant metabolites of F. strobilifera, namely Octylimino dipropan-2-ol, 3,12-diketo-4,6-petromyzonene-24-sulfate, Kaempferol-3-O-rutinoside, Adenosine, and Flavonol 3-O-D-xylosylglucoside, were subjected to molecular docking against InhA (enoyl-acyl carrier protein reductase), a key enzyme involved in mycolic acid biosynthesis. Docking simulations were performed using AutoDock4 following validation through native ligand redocking. In vitro antimycobacterial activity was evaluated against Mycobacterium smegmatis using aqueous, ethanolic, and methanolic leaf extracts at concentrations ranging from 6.25 to 200 mg/mL, with activity assessed by measuring inhibition zone diameters.*
Results: *Molecular docking revealed that 3,12-diketo-4,6-petromyzonene-24-sulfate exhibited the strongest binding affinity toward InhA (−8.90 kcal/mol), slightly surpassing the native ligand (−8.85 kcal/mol), while Flavonol 3-O-D-xylosylglucoside formed multiple hydrogen bonds with key active-site residues (Tyr158, Lys165, and Met199). The latter also formed multiple hydrogen bonds with key active-site residues, including Tyr158, Lys165, and Met199. In vitro evaluation demonstrated concentration-dependent antimycobacterial activity for all extracts. Methanolic extract showed the highest activity, producing inhibition zones ranging from 8.14 ± 0.42 mm to 23.08 ± 0.88 mm, followed by ethanolic extract (7.36 ± 0.38–20.54 ± 0.77 mm) and aqueous extract (5.24 ± 0.31–14.28 ± 0.74 mm). No inhibition was observed in the negative control, while streptomycin sulfate exhibited the highest inhibitory effect.*
Conclusion: *These findings suggest that Flemingia strobilifera represents a promising source of antimycobacterial compounds. Nevertheless, further isolation of the active constituents and validation using pathogenic Mycobacterium tuberculosis as well as in vivo studies are required before therapeutic application can be considered.*

Keywords: Flemingia strobilifera; antimycobacterial activity; InhA; molecular docking; Mycobacterium smegmatis

Introduction

Tuberculosis (TB) remains one of the deadliest infectious diseases worldwide. According to the World Health Organization (WHO), more than 10 million new TB cases are reported annually, with mortality rates remaining particularly high in developing countries. Indonesia ranks second globally in terms of TB burden after India, making TB a major public health concern and a national health priority (Denning, 2024; Gulumbe *et al.*, 2025).

One of the most extensively explored molecular targets in antitubercular drug development is InhA (enoyl-acyl carrier protein reductase), an essential enzyme involved in the biosynthesis of mycolic acids, which are major components of the mycobacterial cell wall

One of the most extensively explored molecular targets in antitubercular drug discovery is InhA (enoyl-acyl carrier protein reductase), an essential enzyme responsible for mycolic acid biosynthesis, a critical component of the mycobacterial cell wall. Inhibition of InhA disrupts cell wall formation, suppressing bacterial growth and survival. Since InhA is also the primary target of isoniazid, it has become one of the most attractive molecular targets for the discovery of novel

antitubercular agents (Alcaraz *et al.*, 2022; Kim *et al.*, 2023; Wang *et al.*, 2023; Harrison *et al.*, 2024; Wahan *et al.*, 2024; Singh *et al.*, 2025; Thakur *et al.*, 2026)

Flemingia strobilifera has been reported to contain a wide range of secondary metabolites with diverse biological activities, including antimicrobial properties (Sirikonda *et al.*, 2023; Sahu *et al.*, 2025). The five dominant metabolites were selected based on our previous LC-HRMS metabolomic profiling of Flemingia strobilifera leaf extract, five dominant compounds—Octylimino dipropan-2-ol, 3,12-diketo-4,6-petromyzonene-24-sulfate, Kaempferol-3-O-rutinoside, Adenosine, and Flavonol 3-O-D-xylosylglucoside—were selected as candidate ligands for evaluating their interactions with InhA through molecular docking analysis. This computational approach enables rapid and efficient prediction of binding affinity and molecular interaction patterns with target proteins prior to further biological validation.

Although *Mycobacterium tuberculosis* is the primary target organism in antitubercular research, its use requires biosafety level-3 (BSL-3) facilities, high operational costs, and extended cultivation periods. Consequently, a safer and more easily cultured model organism is needed for preliminary screening studies. One widely used species is *Mycobacterium smegmatis*, a non-pathogenic, fast-growing *mycobacterium* that shares significant genetic and physiological similarities with *M. tuberculosis* (Sun *et al.*, 2025). Previous studies have demonstrated that *M. smegmatis* possesses an InhA homolog with a high degree of structural and functional conservation, making it a suitable surrogate model for early-stage antitubercular drug discovery (Sparks *et al.*, 2023). The use of M. smegmatis enables a more practical, cost-effective, and safer evaluation of antimycobacterial activity before proceeding to studies involving the actual pathogenic organism.

Based on these considerations, this study aimed to evaluate the antimycobacterial potential of *F. strobilifera* through integrated in silico and in vitro approaches. Molecular docking was employed to predict the interactions of five candidate compounds with InhA, a key enzyme involved in mycobacterial cell wall biosynthesis, while in vitro assays were conducted using leaf extracts against *M. smegmatis* as a preliminary antitubercular screening model. This integrated approach is expected to provide a scientific basis for the development of *F. strobilifera* as a natural source of potential antimycobacterial and antitubercular agents.

Methods

Study Design

This study employed a true experimental design integrating both in silico and in vitro approaches to evaluate the antimycobacterial potential of Otok-otok *(Flemingia strobilifera)* leaf extract. The in silico study was conducted through molecular docking analysis to investigate the interactions of selected phytochemical compounds with the InhA enzyme, while the in vitro study assessed the antimycobacterial activity of the leaf extracts against *Mycobacterium smegmatis* as a preliminary model for antitubercular screening.

Research Site

The study was conducted at the Chemistry and Microbiology Laboratories of STIKES Banyuwangi. Taxonomic identification of Otok-otok *(Flemingia strobilifera)* was carried out at the Biology Laboratory of PGRI University of Banyuwangi to verify the authenticity of the plant material used in this research.

Research Materials

Flemingia strobilifera (Otok-otok) leaves were collected from Licin District, Banyuwangi Regency, East Java, Indonesia, an area traditionally inhabited by the Osing ethnic community. Taxonomic identification was performed at the Biology Laboratory of Universitas Bakti Indonesia (UNIBA) to verify the authenticity of the plant material. A voucher specimen was subsequently deposited in the herbarium for future reference and documentation. The five dominant metabolites were selected based on reported in our previous. Five dominant metabolites were chosen as test ligands, namely Octylimino dipropan-2-ol (L1), 3,12-diketo-4,6-petromyzonene-

24-sulfate (L2), Kaempferol-3-O-rutinoside (L3), Adenosine (L4), and Flavonol 3-O-D-xylosylglucoside (L5). Other materials used in this study included 96% ethanol, Tween 80, Span 80, distilled water, dimethyl sulfoxide (DMSO), Middlebrook 7H9 broth or modified Nutrient Broth for mycobacterial culture, Middlebrook 7H10 agar medium, and Mycobacterium smegmatis culture.

Preparation of Otok-otok Leaf Extracts

The identified *Flemingia strobilifera* leaves were washed thoroughly with running water and air-dried at room temperature until a constant moisture content was achieved. The dried plant material was then ground into a fine powder using a grinder. The powdered simplicia was divided into three portions and extracted separately using distilled water, ethanol, and methanol as solvents. Each extraction was performed by maceration at a sample-to-solvent ratio of 1:10 (w/v) for 72 h at room temperature with periodic stirring. The resulting filtrates were filtered through Whatman No. 1 filter paper and concentrated using a rotary evaporator at 40–50°C for the ethanol and methanol extracts, while the aqueous extract was concentrated using a freeze dryer or a low-temperature vacuum oven. The concentrated extracts were stored at 4°C until further use in antimycobacterial assays.

In Silico Study

The in silico study was conducted using a molecular docking approach to evaluate the interactions of five candidate compounds from *Flemingia strobilifera*—Octylimino dipropan-2-ol, 3,12-diketo-4,6-petromyzonene-24-sulfate, Kaempferol-3-O-rutinoside, Adenosine, and Flavonol 3-O-D-xylosylglucoside—with the target protein InhA (enoyl-acyl carrier protein reductase). The crystal structure of InhA (Mycobacterium tuberculosis) was retrieved from the Protein Data Bank (PDB) ID: 6R9W ,while ligand structures were prepared and energy-minimized prior to docking. Docking protocol validation was performed through redocking of the native ligand to ensure the reliability of the docking parameters. Molecular docking simulations were subsequently carried out using AutoDock4 to determine binding energies and amino acid interaction profiles within the active site of the protein, which were used to predict the antimycobacterial potential of the tested compounds.

In Vitro Study

The antimycobacterial activity of *Flemingia strobilifera* leaf extracts was evaluated against *Mycobacterium smegmatis* using the agar well diffusion method. A bacterial suspension adjusted to the 0.5 McFarland standard was uniformly spread onto the surface of agar media. Aqueous, ethanolic, and methanolic extracts were tested at concentrations of 6.25, 12.5, 25, 50, 100, and 200 mg/mL. Sterile distilled water served as the negative control, while streptomycin sulfate was used as the positive control. A predetermined volume of each extract solution was introduced into wells prepared on the agar surface. The plates were then incubated at 37°C for 24–48 h. Antimycobacterial activity was determined by measuring the diameter of the inhibition zones formed around each well using a digital caliper. All experiments were performed in triplicate, and the results were expressed as mean ± standard deviation.

Data Analysis

The inhibition zone diameters were expressed as mean ± standard deviation (Mean ± SD) from three independent replicates. Data were analyzed descriptively to evaluate the effects of extraction solvents and extract concentrations on antimycobacterial activity. The antimicrobial efficacy of each treatment was compared based on the size of the inhibition zones, and the results were presented in the form of tables and graphs.

Result

Five Dominant Compounds of Flemingia strobilifera as Test Ligands

Table 1. Five Dominant Compounds of *Flemingia strobilifera* Selected as Test Ligands

Ligand Code	Compound Name	Molecular Formula	Compound Class	Main Biological Properties
L1	Octylimino dipropan-2-ol	$C_{11}H_{25}NO_2$	Secondary amine	Polar compound with potential antibacterial activity
L2	3,12-diketo-4,6-petromyzonene-24-sulfate	$C_{27}H_{40}O_8S$	Steroid derivative	Potential bioactive compound with limited previous reports
L3	Kaempferol-3-O-rutinoside	$C_{27}H_{30}O_{16}$	Flavonoid glycoside	Antioxidant and anti-inflammatory activities
L4	Adenosine	$C_{10}H_{13}N_5O_4$	Nucleoside	Immunomodulatory and cardioprotective effects
L5	Flavonol 3-O-D-xylosylglucoside	$C_{27}H_{30}O_{15}$	Flavonoid glycoside	Antioxidant and antimicrobial activities

Native Ligand Redocking Results

Validation of the molecular docking protocol was performed by redocking the native ligand into the active binding pocket of the InhA MTB target protein. The redocking process was conducted to ensure that the selected docking parameters and algorithms were capable of accurately reproducing the binding pose of the native ligand. The redocking results are presented in Table 2, which summarizes the binding energy values and RMSD of the ten best conformations generated during the simulation.

Table 2. Native Ligand Redocking Results

No	Conformation	Binding Energy (kcal/mol)	RMSD (Å)
1	6	-9.59	2.91
2	9	-9.58	2.91
3	4	-9.52	2.92
4	8	-8.85	1.25
5	2	-8.81	1.27
6	10	-8.63	1.76
7	3	-8.62	1.76
8	1	-8.62	1.76
9	7	-8.62	1.74
10	5	-8.80	1.75

Based on the results presented above, an RMSD value below 2.0 Å was obtained for several conformations, indicating that the docking method used was valid and capable of accurately reproducing the binding pose of the native ligand within the protein active site. Therefore, the established docking parameters were considered reliable and subsequently employed for docking the remaining test ligands (L1–L5).

Docking Results of Test Ligands (L1–L5)

The five dominant metabolites identified from *Flemingia strobilifera* were selected as test ligands (L1–L5) and subsequently docked against the target protein InhA MTB. The docking results are presented in Table 3, which includes the binding energy (kcal/mol), inhibition constant (Ki, nM), and amino acid residues involved in hydrogen bond formation.

Table 3. Molecular Interactions of the Native Ligand and Compounds L1–L5

Compounds	Binding energy (kcal/mol)	Inhibition Constant (nM)	H-Bond interaction Residue
L1	-4.97	225690	Gly192; Ile194
L2	-8.90	301.83	-
L3	-7.79	1960	Pro158
L4	-5.42	106490	Gly192; Ile194; Thr196
L5	-8.05	1260	Tyr158; Lys165; Met199

Native	-8.85	325.55	Tyr158

Based on the data presented above, variations in binding affinity and amino acid interactions were observed among the tested ligands. Ligands with more negative binding energy values indicate stronger and more stable interactions with the active site of the target protein. Several ligands were capable of forming hydrogen bonds with specific amino acid residues, which contributed to the stability of the ligand–protein complex. Comparison with the native ligand revealed that one or two compounds exhibited binding affinities comparable to or even better than the native ligand, suggesting their potential as promising candidates for anti-tuberculosis drug development..

Ligand–Protein Interaction Visualization

Ligand–protein interaction visualization was performed to illustrate the binding patterns formed within the active site of the InhA MTB target protein. The analysis was carried out using BIOVIA Discovery Studio Visualizer, which generated two-dimensional interaction maps between the ligands and amino acid residues. The visualization results revealed that each ligand exhibited distinct interaction patterns with the protein target.

1) Native Ligand

The native ligand served as a reference control in the docking study, as it is known to naturally bind within the active pocket of the target protein. Docking analysis showed a binding energy of –8.85 kcal/mol and an inhibition constant of 325.55 nM. A key interaction was observed with the Tyr158 residue, which plays an important role in maintaining the stability of the ligand–protein complex. The low binding energy and the presence of a hydrogen bond with this critical residue confirm the validity of the docking protocol employed and provide a benchmark for evaluating the binding affinity and interaction profiles of the test ligands (L1–L5).

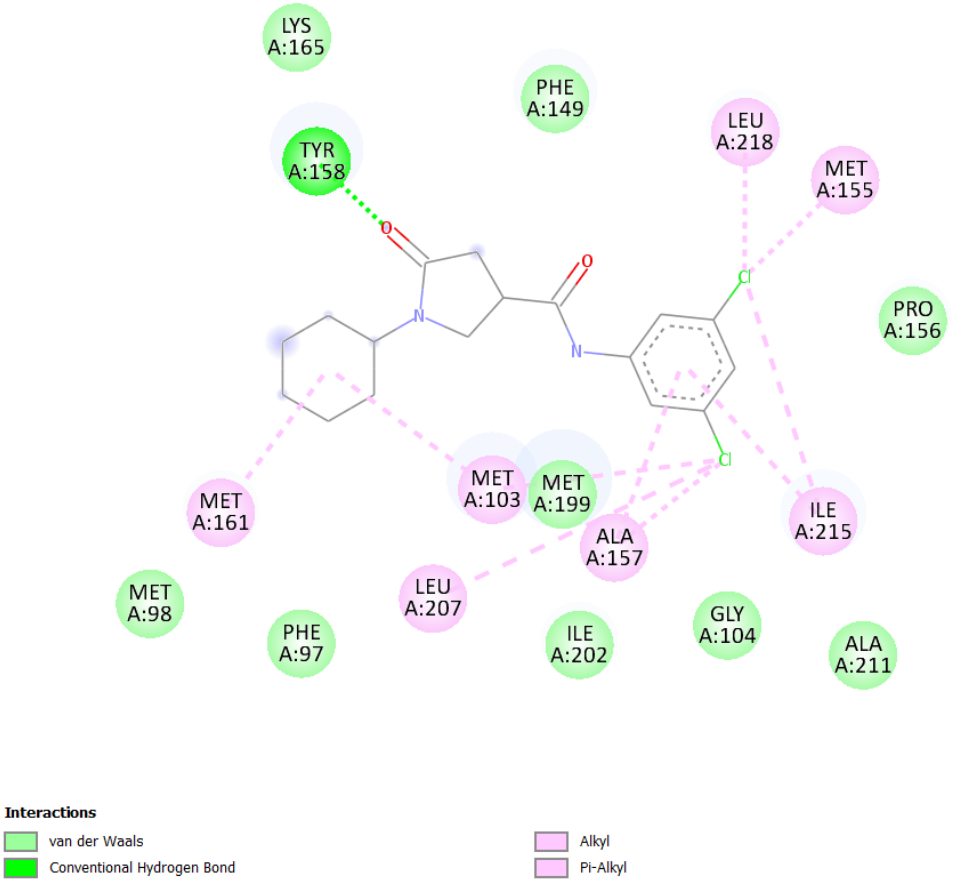

Figure 1. Two-Dimensional Interaction of the Native Ligand and Protein

The interaction visualization of the native ligand in Figure 1 demonstrates the presence of a hydrogen bond with the Tyr158 residue within the protein active site. This interaction pattern

highlights the role of Tyr158 as a key residue in maintaining ligand–protein complex stability and serves as a reference for evaluating the binding characteristics of the other test ligands.

2) Ligand 1 (Octylimino dipropan-2-ol)

L1 exhibited a binding energy of –4.97 kcal/mol with an inhibition constant (Ki) of approximately 225,690 nM. The interaction involved hydrogen bond formation with the Gly192 and Ile194 residues. This binding affinity was relatively weaker than that of the native ligand, indicating that the stability of the L1–protein complex remains insufficient for consideration as a primary candidate inhibitor.

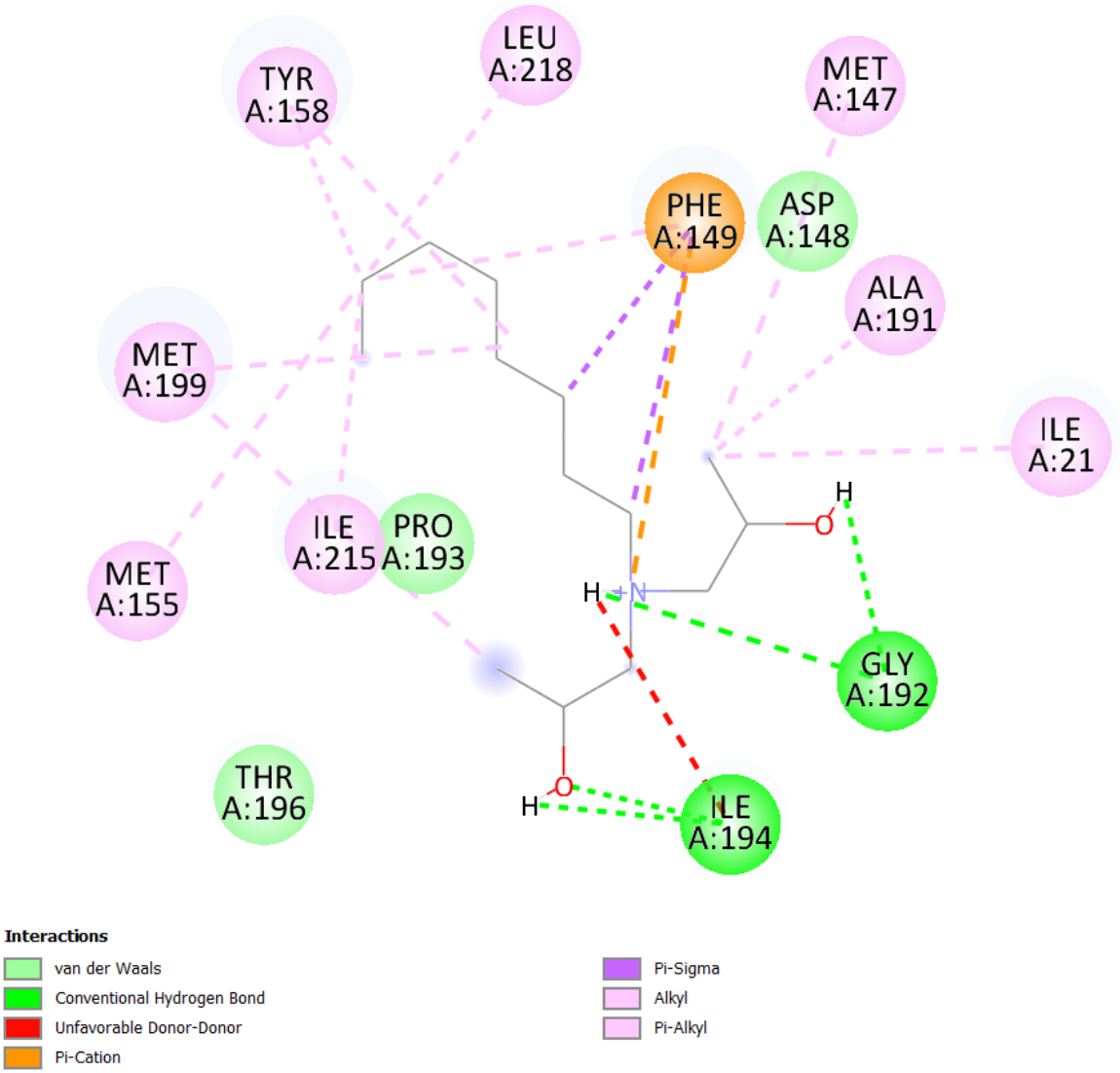

Figure 2. Two-Dimensional Interaction of Ligand 1 and Protein

The two-dimensional interaction analysis of L1 in Figure 2 revealed the formation of hydrogen bonds with the Gly192 and Ile194 residues. However, the interacting residues are located relatively far from the key active-site residues, and the binding position appears weaker compared to that of the native ligand. This observation is consistent with the relatively high binding energy value (–4.97 kcal/mol), indicating that the stability of the L1–protein complex remains limited.

3) Ligand 2 (3,12-diketo-4,6-petromyzonene-24-sulfate)

L2 exhibited the lowest binding energy among all tested ligands, with a value of –8.90 kcal/mol and an inhibition constant of 301.83 nM. Although no specific hydrogen bond interactions with active-site residues were observed, this ligand maintained a highly favorable

binding affinity through hydrophobic interactions and van der Waals forces. Its binding energy was even slightly lower than that of the native ligand, suggesting that L2 may be considered a promising candidate inhibitor.

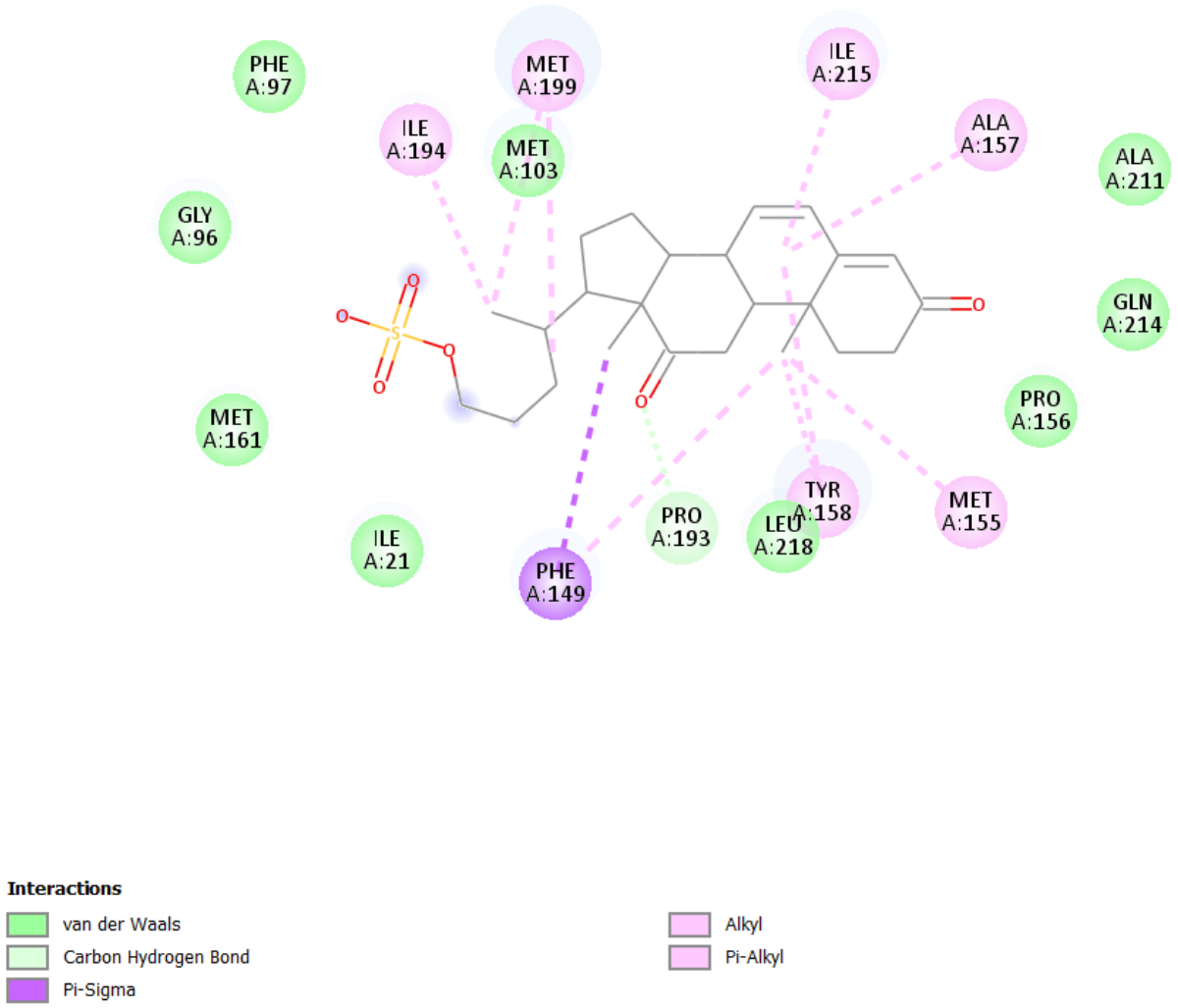

Figure 3. Two-Dimensional Interaction of Ligand 2 and Protein

As shown in Figure 3, L2 did not exhibit specific hydrogen bond formation with the target residues. Nevertheless, its highly favorable binding energy (–8.90 kcal/mol) indicates the presence of strong hydrophobic and van der Waals interactions. This interaction pattern suggests that the ligand is able to stably occupy the active-site pocket despite the absence of direct hydrogen bonding interactions.

4) Ligand 3 (Kaempferol-3-O-rutinoside)

L3 exhibited a binding energy of –7.79 kcal/mol with an inhibition constant of 1,960 nM. The interaction involved the Pro158 residue through hydrogen bond formation. As one of the dominant flavonoid glycosides identified in F. strobilifera, L3 remains a relevant compound for further investigation, although its binding affinity was lower than those of L2 and the native ligand.

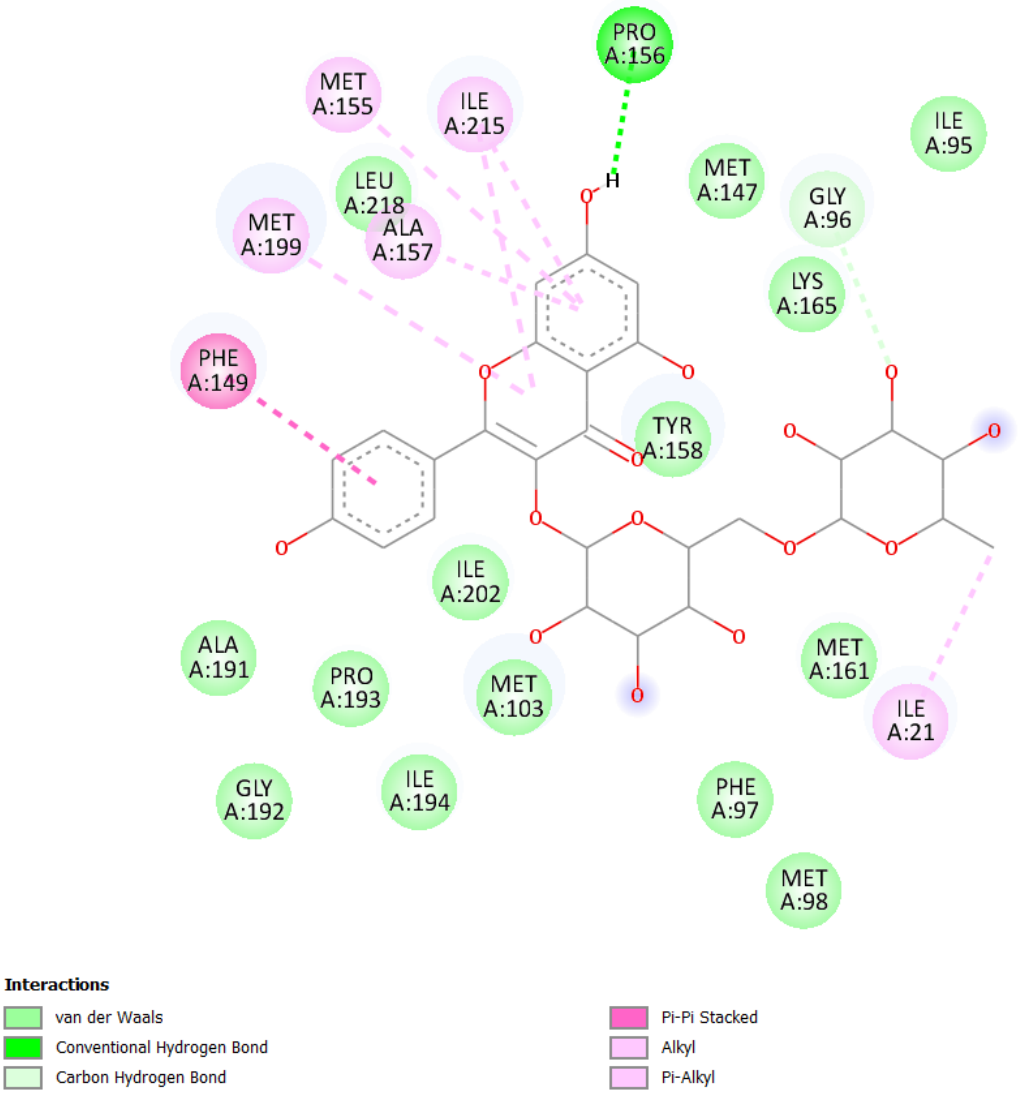

Figure 4. Two-Dimensional Interaction of Ligand 3 and Protein

As illustrated in Figure 5, L3 interacted with the Pro158 residue through hydrogen bond formation. This interaction indicates the ability of the flavonoid ligand to reach a key residue within the active site. The interaction map suggests a relatively stable binding mode, although the binding energy (–7.79 kcal/mol) remained lower than that observed for L2 and the native ligand.

5) Ligand 4 (Adenosine)

L4 exhibited a binding energy of –5.42 kcal/mol with an inhibition constant (Ki) of approximately 106,490 nM. Hydrogen bond interactions were observed with the Gly192, Ile194, and Thr196 residues. Although adenosine was identified as one of the dominant metabolites in the extract, its relatively low binding affinity suggests limited potential as a primary anti-tuberculosis candidate in the present study.

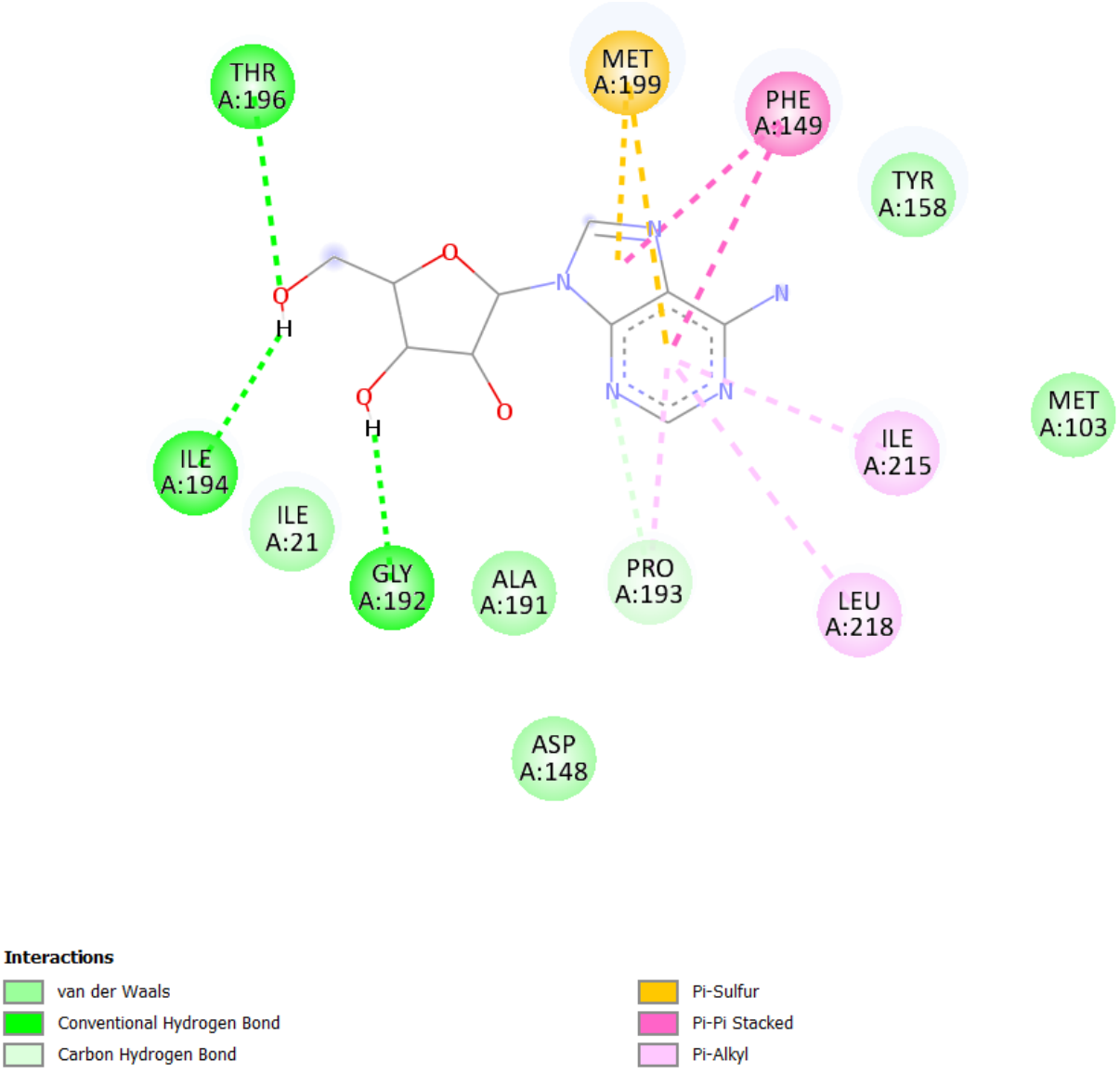

Figure 5. Two-Dimensional Interaction of Ligand 4 and Protein

As shown in Figure 5, L4 interacted with three different residues, namely Gly192, Ile194, and Thr196. The two-dimensional visualization revealed the presence of multiple hydrogen bonds distributed across different regions of the protein active site. Nevertheless, its binding energy (–5.42 kcal/mol) remained higher than those of L3, L5, and L2, indicating a less stable ligand–protein interaction.

6) Ligand 5 (Flavonol 3-O-D-xylosylglucoside)

L5 exhibited a binding energy of –8.05 kcal/mol with an inhibition constant of 1,260 nM. The interaction involved three important residues, namely Tyr158, Lys165, and Met199. This interaction pattern indicates that L5 possesses an attractive combination of relatively strong binding affinity and specific interactions with key active-site residues. Therefore, L5 may be considered a promising candidate for further development as a potential anti-tuberculosis agent.

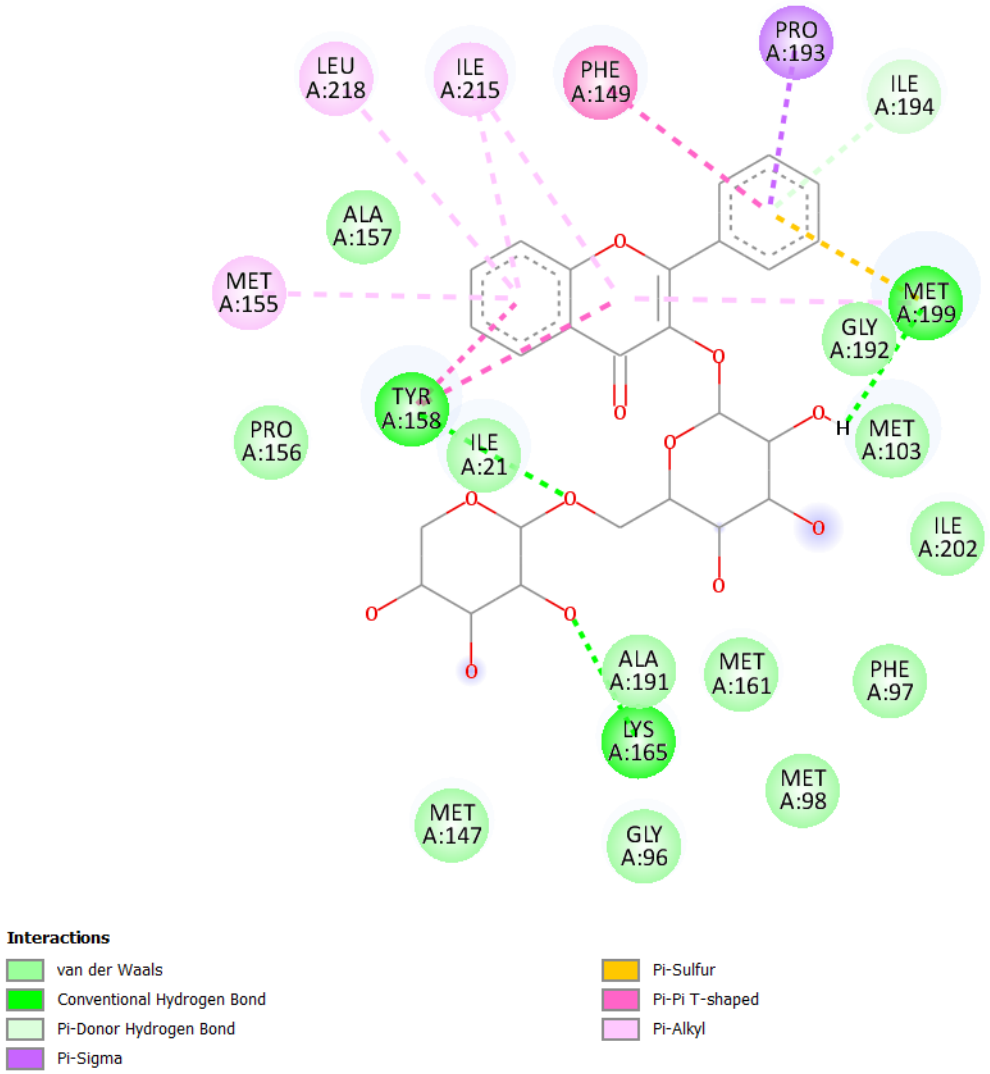

Figure 6. Two-Dimensional Interaction of Ligand 5 and Protein

The two-dimensional interaction analysis of L5 with the target protein in Figure 6 revealed strong and complex hydrogen-bond interactions involving the Tyr158, Lys165, and Met199 residues. This interaction pattern indicates that L5 is capable of interacting with key residues within the protein active site. The combination of multiple hydrogen bonds and a relatively low binding energy (–8.05 kcal/mol) suggests that L5 is one of the most promising candidate compounds identified in this study.

Comparison of Test Ligands with the Native Ligand

The docking results demonstrated variations in binding affinity among the five dominant compounds of *Flemingia strobilifera* when compared with the native ligand. The native ligand exhibited a binding energy of –8.85 kcal/mol and an inhibition constant of 325.55 nM, while interacting with the key residue Tyr158. These characteristics were used as a reference standard for evaluating the binding potential of the test ligands.

Among the tested compounds, L2 (3,12-diketo-4,6-petromyzonene-24-sulfate) displayed a binding affinity comparable to, and slightly better than, that of the native ligand (–8.90 vs. –8.85 kcal/mol). This finding suggests that L2 possesses a highly stable binding capability despite the absence of specific hydrogen-bond interactions. Meanwhile, L5 (Flavonol 3-O-D-xylosylglucoside) also demonstrated promising results, with a binding energy of –8.05 kcal/mol and hydrogen-bond interactions involving three key residues (Tyr158, Lys165, and Met199), which may contribute to its biological activity. L3 (Kaempferol-3-O-rutinoside) showed moderate

affinity (–7.79 kcal/mol) through interaction with the Pro158 residue, indicating its potential relevance for further investigation, which is relevant as one of the protein binding pathways. In contrast, L1 (Octylimino dipropan-2-ol) and L4 (Adenosine) displayed lower binding affinity values (–4.97 and –5.42 kcal/mol, respectively), indicating that their contributions as primary candidate inhibitors are relatively limited.

Antimycobacterial Activity Assay Results

Table 4. Inhibition Zone Diameter of *Flemingia strobilifera* Extracts Against *Mycobacterium smegmatis*

Concentration	Inhibition Zone (mm) Mean ± SD		
	F. strobilifera **Aqueous Extract**	***F. strobilifera*** **Ethanolic Extract**	***F. strobilifera*** **Methanolic Extract**
Negative Control (NC, Sterile Water)	0.00 ± 0.00	0.00 ± 0.00	0.00 ± 0.00
6.25 mg/mL	0.00 ± 0.00	0.00 ± 0.00	8.14 ± 0.42
12.5 mg/mL	0.00 ± 0.00	7.36 ± 0.38	10.58 ± 0.51
25 mg/mL	6.82 ± 0.41	10.21 ± 0.47	12.84 ± 0.56
50 mg/mL	8.97 ± 0.52	13.68 ± 0.58	15.71 ± 0.65
100 mg/mL	11.74 ± 0.63	17.02 ± 0.69	19.46 ± 0.79
200 mg/mL	14.28 ± 0.74	20.54 ± 0.77	23.08 ± 0.88
Positive Control (PC, *Streptomycin Sulfate*)	26.12 ± 0.46	26.12 ± 0.46	26.12 ± 0.46

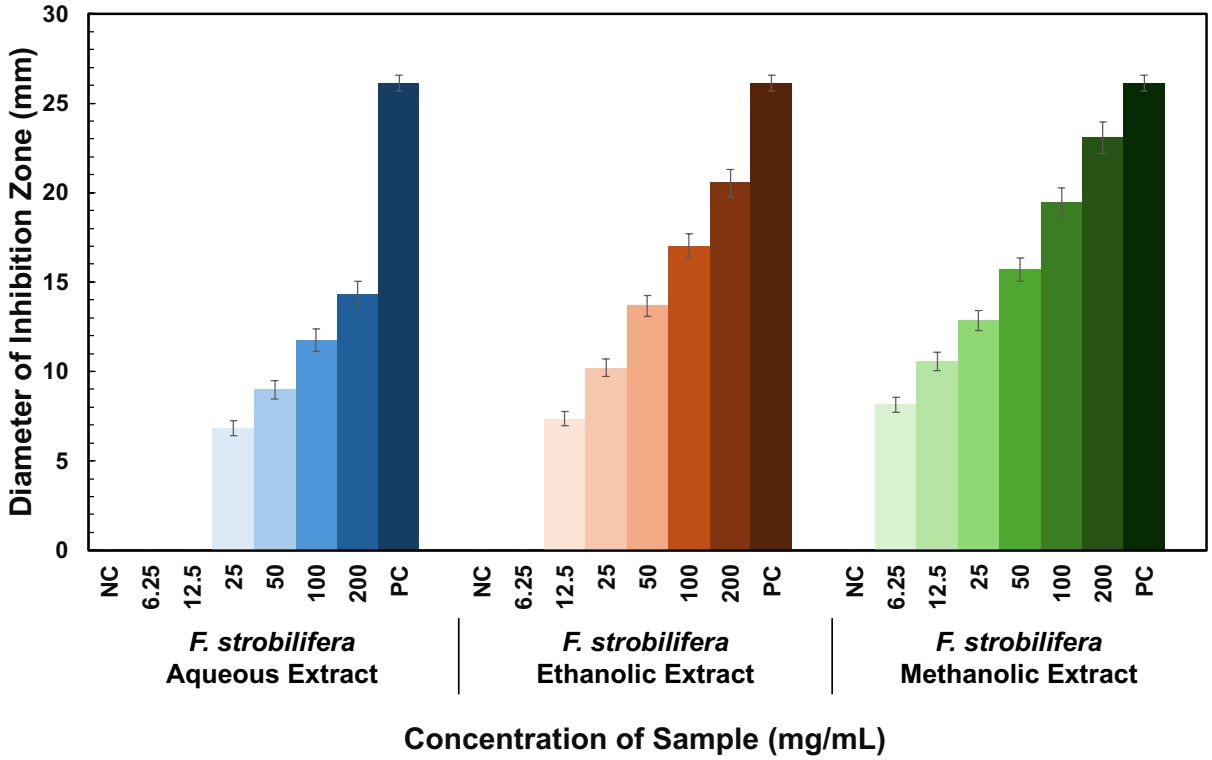

Figure 7. Antimicrobial assay of *F. strobilifera* aqueous extract, *F. strobilifera* ethanolic extract, *F. strobilifera* methanolic extract againts *M. smegmatis*

The antimycobacterial activity assay demonstrated that all *Flemingia strobilifera* leaf extracts were capable of inhibiting the growth of *Mycobacterium smegmatis*, with inhibitory activity increasing in a concentration-dependent manner. The methanolic extract exhibited the

highest activity among all tested extracts, with inhibition zone diameters increasing from 8.14 ± 0.42 mm at 6.25 mg/mL to 23.08 ± 0.88 mm at 200 mg/mL. The ethanolic extract showed the second-highest activity, producing inhibition zones ranging from 7.36 ± 0.38 mm to 20.54 ± 0.77 mm, whereas the aqueous extract exhibited the lowest activity, with a maximum inhibition zone of 14.28 ± 0.74 mm at 200 mg/mL. No inhibition zone was observed in the negative control, indicating that the solvent itself did not exert antimycobacterial effects, while the positive control, streptomycin sulfate, produced an inhibition zone of 26.12 ± 0.46 mm. These findings suggest that the antimycobacterial bioactive compounds present in *F. strobilifera* leaves are more efficiently extracted using organic solvents, particularly methanol, and that the inhibitory activity is concentration-dependent.

Discussion

The docking results revealed variations in binding affinity and residue interaction patterns among the five dominant compounds of *Flemingia strobilifera* against InhA (enoyl-acyl carrier protein reductase) of *Mycobacterium tuberculosis*, a key enzyme involved in the biosynthesis of mycolic acids in the bacterial cell wall. InhA is recognized as a primary target of isoniazid, and inhibition of this enzyme can disrupt the integrity of the *M. tuberculosis* cell wall, ultimately suppressing bacterial growth. (EL Haddoumi *et al.*, 2023; Wahan *et al.*, 2024; Rizet *et al.*, 2025).

Among the tested compounds, 3,12-diketo-4,6-petromyzonene-24-sulfate (L2) exhibited the most favorable binding energy (–8.90 kcal/mol), which was even lower than that of the native ligand (–8.85 kcal/mol). Although L2 did not form hydrogen bonds with specific amino acid residues, strong hydrophobic interactions and van der Waals forces within the active pocket of InhA MTB contributed substantially to the stability of its binding. This finding highlights that ligands with low binding energy values may still possess high inhibitory potential even in the absence of explicit hydrogen-bond interactions. Meanwhile, Flavonol 3-O-D-xylosylglucoside (L5) also demonstrated notable activity, with a binding energy of –8.05 kcal/mol and the formation of multiple hydrogen bonds with key InhA MTB residues, namely Tyr158, Lys165, and Met199. This interaction pattern is particularly important because ligands capable of interacting with critical residues within the active site generally exhibit greater stability and selectivity in enzyme inhibition. Therefore, L5 not only displayed high binding affinity but also showed specific interactions that support its potential as an InhA MTB inhibitor. Although the molecular docking identified L2 and L5 as the compounds with the highest affinity toward InhA, the antimycobacterial activity observed in the crude extracts cannot be attributed solely to these compounds. The extract contains numerous secondary metabolites that may exert antibacterial activity through multiple mechanisms, including disruption of membrane integrity, inhibition of other enzymes, or synergistic interactions among phytochemicals. Therefore, the docking results should be interpreted as predictive evidence rather than direct mechanistic confirmation.

Another flavonoid, Kaempferol-3-O-rutinoside (L3), exhibited interaction with the Pro158 residue and showed moderate binding affinity (–7.79 kcal/mol). This observation is consistent with previous reports indicating that flavonoids can inhibit various bacterial enzymes through interactions with active-site residues and the induction of oxidative stress (Rabaan *et al.*, 2022; do Nascimento and da Costa, 2025; Luo *et al.*, 2025; Zhang *et al.*, 2025). Although its affinity was lower than those of L2 and L5, L3 remains relevant as a bioactive candidate that may contribute to synergistic effects. In contrast, Adenosine (L4) and Octylimino dipropan-2-ol (L1) exhibited lower binding affinities, with values of –5.42 and –4.97 kcal/mol, respectively. Although adenosine formed several hydrogen bonds with Gly192, Ile194, and Thr196, these interactions were insufficient to stabilize its binding with InhA MTB. This finding emphasizes that the abundance of a metabolite in a plant extract does not necessarily correlate with its bioactivity against a specific molecular target.

Overall, these findings indicate that effective ligands for InhA MTB inhibition are characterized by two main features: (i) low binding energy values, which reflect stable ligand–protein interactions, and (ii) involvement of key residues within the active site, which directly contribute to enzyme inhibition. Based on these criteria, L2 and L5 can be considered the most

promising candidates identified from *Flemingia strobilifera*. Furthermore, this study demonstrates that the integration of metabolomic analysis with in silico docking can effectively guide the identification of dominant compounds with potential pharmacological activity against tuberculosis. Nevertheless, the present in silico findings remain predictive in nature. Therefore, further in vitro and in vivo studies are required to validate the biological activity and assess the safety of these compounds, thereby supporting the development of InhA MTB inhibitor candidates derived from *F. strobilifera*.

In the in vitro assay, the antimycobacterial activity of *Flemingia strobilifera* leaf extracts against *Mycobacterium smegmatis* exhibited a concentration-dependent pattern, as evidenced by the increase in inhibition zone diameter with increasing extract concentration. Among the three types of extracts tested, the concentration of 200 mg/mL produced the highest inhibitory activity. These results suggest that higher extract concentrations allow greater amounts of bioactive compounds to diffuse into the medium and interact with bacterial cells, thereby enhancing growth inhibition. The absence of inhibition zones in the negative control indicates that the observed antimicrobial effect originated from the active compounds present in the extracts, whereas the positive control, streptomycin sulfate, exhibited the strongest antimycobacterial activity and served as the reference standard.

The differences in antimycobacterial activity among the various extracts indicate that the extraction solvent significantly influences both the quantity and types of secondary metabolites recovered. The antimycobacterial activity observed in the present study is comparable with, and in some cases exceeds, that reported for several medicinal plant extracts tested against Mycobacterium smegmatis. For example, methanolic extract of Martynia annua produced inhibition zones of approximately 19 mm at 100 mg/mL, whereas Aloe vera and Ocimum tenuiflorum exhibited considerably lower inhibition zones of approximately 12.5 mm and 9.1 mm, respectively. In comparison, the methanolic extract of Flemingia strobilifera produced an inhibition zone of 23.08 ± 0.88 mm at 200 mg/mL, indicating relatively strong antimycobacterial activity among crude plant extracts evaluated using diffusion-based assays. The methanolic extract produced the largest inhibition zones at all tested concentrations, followed by the ethanolic and aqueous extracts. These findings suggest that most of the antimycobacterial compounds present in *F. strobilifera* leaves exhibit greater solubility in organic solvents than in polar solvents such as water. The observed activity is likely associated with the presence of flavonoids and other bioactive metabolites known to disrupt cell wall integrity, inhibit essential enzymatic functions, and interfere with mycobacterial metabolic processes. (Dyba *et al.*, 2025; Liu *et al.*, 2025; Yang *et al.*, 2026). These results are consistent with the in silico findings, which identified several compounds from *F. strobilifera* with favorable affinity toward the InhA target, suggesting that this plant has considerable potential as a source of candidate antimycobacterial agents for further investigation.

To better contextualize the present findings, the antimycobacterial activity of *Flemingia strobilifera* was compared with previous studies evaluating medicinal plant extracts against *Mycobacterium smegmatis.* Several reports have demonstrated that crude plant extracts generally produce inhibition zones ranging from approximately 8–20 mm depending on the plant species, extraction solvent, concentration, and assay conditions. For instance, ethanolic extract of Clerodendrum minahassae exhibited inhibition zones of approximately 9–11 mm against M. smegmatis, whereas methanolic extract of Martynia annua produced inhibition zones approaching 19 mm at comparable concentrations. In the present study, the methanolic extract of *F. strobilifera* produced an inhibition zone of 23.08 ± 0.88 mm at 200 mg/mL, indicating relatively strong antimycobacterial activity among crude plant extracts evaluated using agar diffusion assays. Nevertheless, direct comparisons should be interpreted with caution because inhibition zone diameters are influenced by multiple experimental variables, including extraction procedures, phytochemical composition, extract concentration, solvent system, diffusion characteristics, bacterial inoculum density, and culture media. Overall, these comparisons support the promising antimycobacterial potential of *F. strobilifera* while emphasizing the need

for further studies involving bioassay-guided fractionation, minimum inhibitory concentration (MIC) determination, and validation against pathogenic *Mycobacterium tuberculosis*.

Conclusion

This study demonstrated that *Flemingia strobilifera* possesses significant potential as a source of antimycobacterial compounds, as evidenced by both in silico and in vitro approaches. Molecular docking analysis identified 3,12-diketo-4,6-petromyzonene-24-sulfate (L2) and Flavonol 3-O-D-xylosylglucoside (L5) as the most promising InhA inhibitor candidates, characterized by high binding affinity and favorable interactions within the enzyme's active site. Furthermore, in vitro assays against *Mycobacterium smegmatis* revealed that *F. strobilifera* leaf extracts exhibited concentration-dependent antimycobacterial activity, with the methanolic extract producing the largest inhibition zones compared to the ethanolic and aqueous extracts. These findings suggest that the bioactive metabolites present in *F. strobilifera* may contribute to the inhibition of mycobacterial growth, highlighting the potential of this plant as a source of candidate antitubercular agents. Further investigations, including in vivo studies and more comprehensive mechanistic analyses, are warranted to validate its therapeutic potential.

SUGGESTIONS

The present study demonstrated the antimycobacterial potential of *Flemingia strobilifera* through integrated in silico and in vitro approaches. Further studies are recommended to isolate and characterize the active compounds responsible for the observed biological activity.

ACKNOWLEDGMENT

The authors gratefully acknowledge the Directorate of Research, Ministry of Higher Education, Science, and Technology of the Republic of Indonesia for the financial support through the 2025 Beginner Lecturer Research Grant (PDP). This research was funded under Contract Numbers 128/C3/DT.05.00/PL/2025, 143/LL7/DT.05.00/PL/2025, and 184b/05/STIKES BWI/VI/2025. The authors sincerely appreciate the support, guidance, and resources provided, which were essential for the successful completion of this study.

DECLARATION OF INTEREST

The authors declare that there are no conflicts of interest regarding the publication of this study.

FUNDING

This research was funded by the Directorate of Research, Ministry of Higher Education, Science, and Technology of the Republic of Indonesia through the 2025 Beginner Lecturer Research Grant (PDP). Financial support was provided under Contract Numbers 128/C3/DT.05.00/PL/2025, 143/LL7/DT.05.00/PL/2025, and 184b/05/STIKES BWI/VI/2025.

REFERENCES

Alcaraz, M. *et al.* (2022) 'Designing quinoline-isoniazid hybrids as potent anti-tubercular agents inhibiting mycolic acid biosynthesis', *European Journal of Medicinal Chemistry*, 239, p. 114531. Available at: https://doi.org/https://doi.org/10.1016/j.ejmech.2022.114531.

Denning, D.W. (2024) 'Global incidence and mortality of severe fungal disease', *The Lancet Infectious Diseases*, 24(7), pp. e428–e438. Available at: https://doi.org/10.1016/S1473-3099(23)00692-8.

Dyba, B. *et al.* (2025) 'The effects of 3-hydroxyflavone complexes with transition metal ions on the physicochemical and microbial properties of bacterial cell membranes', *Scientific Reports*, 15(1), p. 20743. Available at: https://doi.org/10.1038/s41598-025-07358-y.

Gulumbe, B.H. *et al.* (2025) 'WHO report signals tuberculosis resurgence: Addressing systemic failures and revamping control strategies', *Decoding Infection and Transmission*, 3, p. 100044.

Available at: https://doi.org/https://doi.org/10.1016/j.dcit.2025.100044.
EL Haddoumi, G. *et al.* (2023) 'Facing Antitubercular Resistance: Identification of Potential Direct Inhibitors Targeting InhA Enzyme and Generation of 3D-pharmacophore Model by in silico Approach', *Advances and Applications in Bioinformatics and Chemistry*, 16(null), pp. 49–59. Available at: https://doi.org/10.2147/AABC.S394535.
Harrison, G.A. *et al.* (2024) 'Inducing vulnerability to InhA inhibition restores isoniazid susceptibility in drug-resistant *Mycobacterium tuberculosis*', *mBio*, 15(3), pp. e02968-23. Available at: https://doi.org/10.1128/mbio.02968-23.
Kim, S.K. *et al.* (2023) 'Structure and dynamics of the essential endogenous mycobacterial polyketide synthase Pks13', *Nature Structural & Molecular Biology*, 30(3), pp. 296–308. Available at: https://doi.org/10.1038/s41594-022-00918-0.
Liu, Y. *et al.* (2025) 'Flavonoids as Promising Natural Compounds for Combating Bacterial Infections', *International Journal of Molecular Sciences*, 26(6), p. 2455. Available at: https://doi.org/10.3390/ijms26062455.
Luo, Jincan *et al.* (2025) 'Latest research progress on anti-microbial effects, mechanisms of action, and product developments of dietary flavonoids: A systematic literature review', *Trends in Food Science & Technology*, 156, p. 104839. Available at: https://doi.org/10.1016/j.tifs.2024.104839.
do Nascimento, J.B. and da Costa, J.G.M. (2025) 'Flavonoids: A Review of Antibacterial Activity Against Gram-Negative Bacteria', *International Journal of Microbiology*. Edited by E. Saini, 2025(1). Available at: https://doi.org/10.1155/ijm/9961121.
Rabaan, A.A. *et al.* (2022) 'Promising Antimycobacterial Activities of Flavonoids against Mycobacterium sp. Drug Targets: A Comprehensive Review.', *Molecules (Basel, Switzerland)*, 27(16). Available at: https://doi.org/10.3390/molecules27165335.
Rizet, J. *et al.* (2025) 'Is Mycobacterial InhA a Suitable Target for Rational Drug Design?', *ChemMedChem*, 20(13). Available at: https://doi.org/10.1002/cmdc.202500079.
Sahu, A. *et al.* (2025) 'Flemingia Strobilifera– An Updated Review on its Pharmacognostic and Pharmacological Properties', *Current Nutrition & Food Science*, 21(4), pp. 421–429. Available at: https://doi.org/10.2174/0115734013313350240918050329.
Singh, J. *et al.* (2025) 'Targeting Mycobacterium tuberculosis InhA with Phytochemicals : Insights from Molecular Docking and Dynamics Simulations', *Journal of Pure and Applied Microbiology*, 19(April), pp. 2305–2321. Available at: https://doi.org/10.22207/JPAM.19.3.56.
Sirikonda, A. *et al.* (2023) 'Micropropagation of 2-methoxy-4-vinyl phenol rich Flemingia strobilifera and assessment of genetic and biochemical fidelity by SCoT and GC-MS analysis', *Plant Cell, Tissue and Organ Culture (PCTOC)*, 154(3), pp. 541–550. Available at: https://doi.org/10.1007/s11240-023-02526-2.
Sparks, I.L. *et al.* (2023) 'Mycobacterium smegmatis : The Vanguard of Mycobacterial', *Journal of Bacteriology*, 205(1), pp. 1–16.
Sun, H. *et al.* (2025) 'Transcriptomic Analysis of Macrophages Infected with Mycobacterium smegmatis', *Microbiology Research*, p. 146. Available at: https://doi.org/10.3390/microbiolres16070146.
Thakur, M. *et al.* (2026) 'Molecular and pharmacological impacts of phytochemicals on the enoyl-acyl carrier protein reductase: potential therapeutic implications in tuberculosis', *Integrative Biology*, 18, p. zyag007. Available at: https://doi.org/10.1093/intbio/zyag007.
Wahan, S.K. *et al.* (2024) 'Unlocking InhA: Novel approaches to inhibit Mycobacterium tuberculosis', *Bioorganic Chemistry*, 146, p. 107250. Available at: https://doi.org/https://doi.org/10.1016/j.bioorg.2024.107250.
Wang, K. *et al.* (2023) 'PatA Regulates Isoniazid Resistance by Mediating Mycolic Acid Synthesis and Controls Bio fi lm Formation by Affecting Lipid Synthesis in Mycobacteria', *microbiology spectrum*, 11(3), pp. 1–12.
Yang, T. *et al.* (2026) 'Barley Flavonoids: Molecular Insights into Disease Resistance and Stress Tolerance for Sustainable Agriculture', *Journal of Plant Growth Regulation*, 45(3), pp. 1677–1696. Available at: https://doi.org/10.1007/s00344-025-11997-w.

Zhang, Z. *et al.* (2025) 'Research Progress on the Antibacterial Activity of Natural Flavonoids', *Antibiotics*. Available at: https://doi.org/10.3390/antibiotics14040334.